Article

Evaluation of Substituted *N*-Aryl Maleimide and Acrylamides for Bioconjugation

Hugh G. Hiscocks [1], Giancarlo Pascali [2,3,4,*] and Alison T. Ung [1]

1 School of Mathematical and Physical Sciences, Faculty of Science, University of Technology Sydney, Broadway, Sydney, NSW 2007, Australia; hugh.hiscocks@uts.edu.au (H.G.H.); alison.ung@uts.edu.au (A.T.U.)
2 School of Chemistry, University of New South Wales, Kensington, NSW 2052, Australia
3 Australian Nuclear Science and Technology Organisation, Lucas Heights, NSW 2234, Australia
4 Faculty of Medicine and Health, University of Sydney, Camperdown, NSW 2050, Australia
* Correspondence: g.pascali@unsw.edu.au

Abstract: Novel SF_5-bearing maleimide and acrylamide derivatives were synthesised as potential [^{18}F]radio-prosthetic groups for radiolabelling peptides and proteins. The efficacy of selected prosthetic groups was first assessed through bioconjugation with protected model amino acid derivatives. These reactions were investigated on an analytical scale via LC-MS across a pH range to quantitatively evaluate this prosthetic group's reactivity and stability. Model bioconjugate reactions were then replicated using analogous *para*-substituted derivatives to determine the influence of the electronic effects of -SF_5. Finally, the SF_5-bearing prosthetic groups were utilised for bioconjugation with cancer-targeting c-RGD peptides. *N*-aryl maleimides reacted extremely efficiently with the model amino acid *N*-acetyl-*L*-cysteine. The subsequent conjugates were obtained as regio-isomeric mixtures of the corresponding thio-succinamic acids in yields of 80–96%. Monitoring the bioconjugate reaction by LC-MS revealed that ring hydrolysis of the intermediate SF_5–thio-succinimide conjugate occurred instantaneously, an advantageous quality in minimising undesirable thiol exchange reactions with non-targeted cysteine residues. In contrast, *N*-aryl acrylamides demonstrated poor solubility in semi-aqueous media (<1 mM). In turn, synthetic-scale model bioconjugations with N_α-acetyl-*L*-lysine were performed in methanol, affording the corresponding acrylamide conjugates in modest to high yield (58–89%). Including electron-deficient, fluorinated prosthetic groups for bioconjugation will broaden their applicability within the fields of ^{19}F-MRI and PET imaging.

Keywords: bioconjugation; sulfur pentafluoride; maleimide; acrylamide

1. Introduction

Bioconjugation is the coupling of a biologically active molecule, such as a peptide, protein or antibody, with a fragment bearing a particular function, such as a drug, nanoparticle, fluorescent tag or radiolabel. Conjugation between the two components is achieved via an intermediary covalent linkage established by a reactive and chemo-selective prosthetic group (Scheme 1); it is, however, appropriate to speak of "bioconjugation" when the reaction conditions are compatible with the use of biologics (e.g., aqueous buffer conditions).

Our group has previously demonstrated that the 3- and 4-nitrophenyl sulphur pentafluoride can undergo ^{18}F/^{19}F radioisotopic exchange [1]. In addition to its potential as an [^{18}F]F radio-synthon, the -SF_5 group also demonstrates unique pharmacological properties owing to its high lipophilicity ($\pi = 1.51$, relative to the –CF_3 group; $\pi = 1.09$) and electron withdrawing effect ($\sigma_p = 0.68$, relative to the –CF_3 group; $\sigma_p = 0.54$) [2,3]. Furthermore, the groups high fluorine content shows promise for its potential application as an ^{19}F-MRI tag [4].

= Drug, Radiolabel, Fluorescent tag etc.
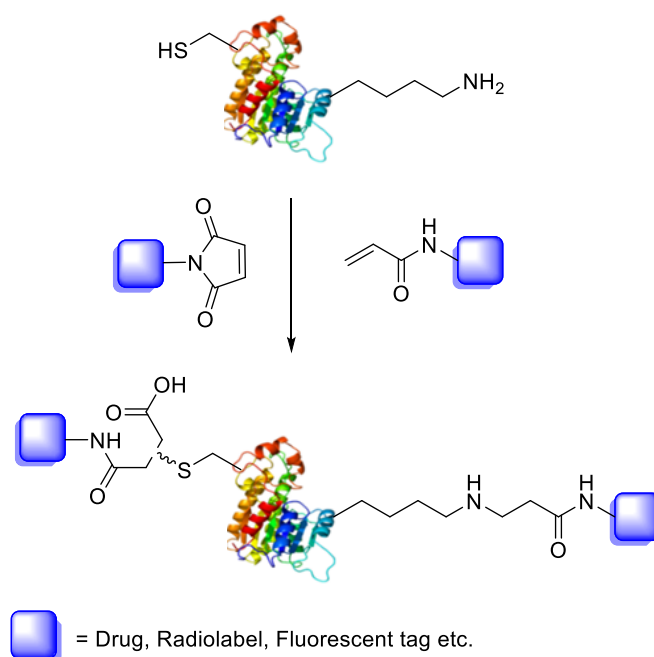
Scheme 1. Bioconjugation of protein or peptide with a drug, radiolabel or fluorescent tag through either maleimide or acrylamide prosthetic groups.

In light of these attributes, we investigated the PTAD–tyrosine conjugation as a potential means of selectively introducing an -[^{18}F]SF$_5$ tag onto the side chains of tyrosine residues [5]. However, it was found that the aqueous stability of the SF$_5$-bearing PTAD derivative was a significant limitation and could only be used for bio-conjugation successfully under highly specialised conditions. For this reason, our investigation changed focus to the more robust maleimide and acrylamide moieties for selective bioconjugation with cysteine and lysine residues, respectively.

The thiol side chain of cysteine residues is a common target for bioconjugate reactions due to the unique nucleophilicity of the thiolate anion and its relatively low abundance in peptides and proteins [6]. This abundance enables selective bioconjugation to be performed with a high degree of chemo- and regio-selectivity with the appropriate prosthetic group. Maleimides have been used extensively as prosthetic groups for cysteine selective bioconjugation, owing to their fast rate kinetics, selectivity and lack of by-products. The impressive selectivity of the maleimide towards thiols is imparted in two ways: firstly, the pKa of the thiol group (cysteine intrinsic pKa = ~8.6) allows for reactions to be performed in a pH range of 6.5–7.5, whereby potentially competing side chains, such as the ε-amine of lysine residues, remain predominantly protonated and thus unreactive [7].

A major limitation of maleimide–cysteine conjugation is the propensity for the intermediate thio-succinimide ether to undergo β-elimination through the action of either base or nucleophile [8]. This regenerates the maleimide, which can consequently undergo conjugation to non-targeted endogenous biomolecules, presenting a significant issue for in vitro applications such as PET imaging of biomolecule–radiolabel conjugates (Scheme 2). Thiol exchange has been sparingly reported in the literature. For example, Alley et al. observed thiol exchange by mass spectrometry between thio-succinimide-linked antibody–drug conjugates and rat serum albumin in vivo, consequently forming albumin–drug conjugates [9]. Lewis et al. utilised a *bis*-maleimide linker to conjugate a monoclonal antibody with a DOTA chelating agent for radiolabelling with ^{111}In(III) and ^{90}Y(III); much like Alley et al., the authors observed that the conjugate underwent significant thiol exchange with human serum albumin in vivo [10].
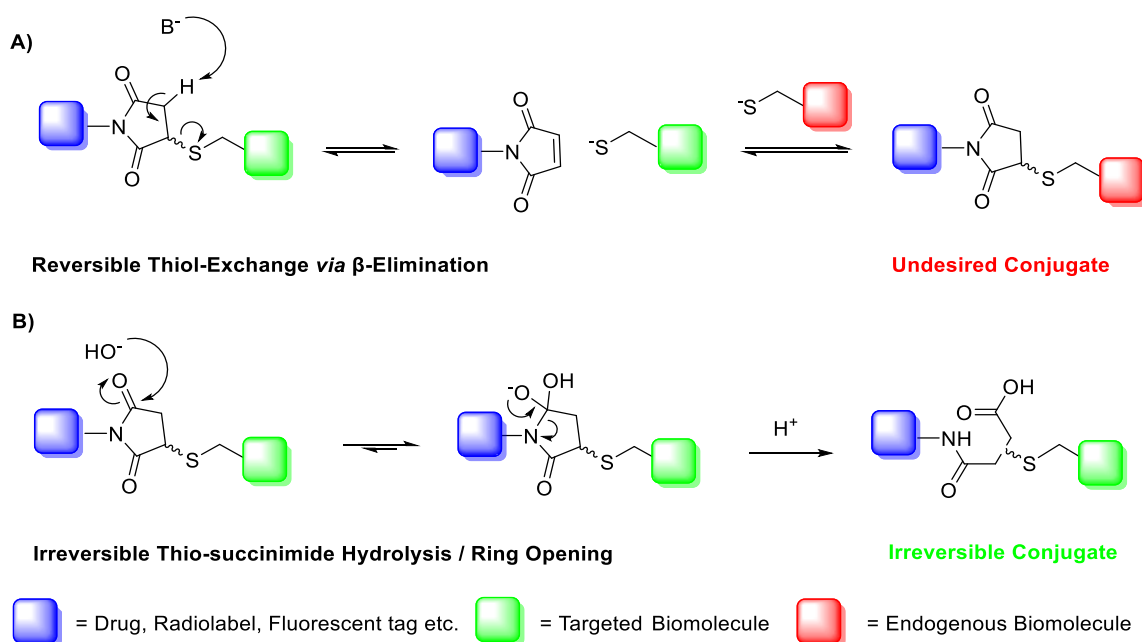
Scheme 2. (**A**) Base- or thiolate-induced β-elimination of the thio-succinimide conjugate and subsequent thiol exchange. (**B**) Irreversible aqueous hydrolysis of the thio-succinimide ring to the corresponding regio-isomeric thio-succinamic acids.

The propensity for the thio-succinimide ether to undergo β-elimination and subsequent thiol exchange is driven by the acidity of the α proton, which is increased by electron-withdrawing groups. On the other hand, this same electron-withdrawing effect also increases the electrophilicity of the carbonyl carbons, thus encouraging ring hydrolysis to a stable and irreversible thio-succinamic acid conjugate, a well-documented occurrence [11–13]. The influence of electronic effects on thio-succinimide conjugate stability was first reported by Baldwin et al. in 2011, who found that electron-withdrawing substituents increase the rate constant for thio-succinimide ring opening, thus minimising the conjugates susceptibility towards thiol exchange [14]. This affect was investigated further by Fontaine et al., who deduced the rate constants for these competing reactions across a wide variety of substituted *N*-aliphatic maleimides [15]. It was found that favourability for thio-succinimide ring hydrolysis over thiol exchange at pH = 7.4 was significantly improved with increasingly electron-withdrawing *N*-alkyl substituents, indicating that electron-withdrawing groups are ultimately beneficial in preventing thiol exchange.

In 2014, an alternative approach was utilised by Lyon and co-workers for inducing thio-succinimide ring hydrolysis, whereby a diaminopropionic acid linker was utilised between the maleimide head group and drug payload, the primary amine of which was found to act as an intermolecular catalyst to rapidly induce ring hydrolysis in the subsequent thio-succinimide antibody–drug conjugates [16]. Later, in 2015, Christie et al. evaluated the stability of a variety of antibody–drug conjugates formed via maleimides bearing either *N*-aryl or *N*-alkyl linkers. From their results, researchers observed substantially faster rates of thio-succinimide ring hydrolysis among the *N*-aryl maleimide conjugates [13]. Furthermore, the researchers found that the *N*-aryl maleimide derivatives reacted approximately 2.5 times faster with the thiolate substrates compared with the *N*-alkyl derivatives investigated, a desirable quality for time-sensitive applications such as ^{18}F-radiolabelling.

In light of these findings, we set out to determine if an aryl -SF$_5$ moiety would promote thio-succinimide ring hydrolysis in addition to serving as an efficient means of tagging cysteine residues with the -SF$_5$ group for ^{19}F-MRI or PET applications. For this reason, 4-[4-(pentafluorosulfanyl)phenyl]pyrrole-2,5-dione (**2a**) was envisaged as a potential prosthetic group for incorporating the -SF$_5$ moiety onto biomolecules of interest (Figure 1).
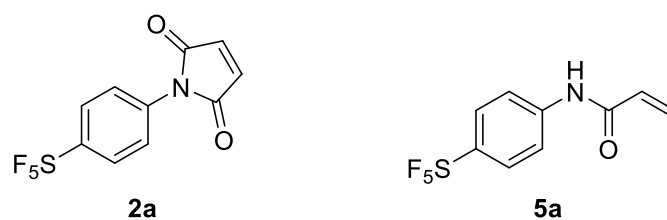
Figure 1. Selected -SF$_5$ prosthetic groups for bioconjugation: 4-[4-(pentafluorosulfanyl) phenyl]pyrrole-2,5-dione (**2a**) and 4-[4-(pentafluorosulfanyl)phenyl]-2-propenamide (**5a**).

Due to the susceptibility of maleimides towards alkaline hydrolysis, they are substantially less applicable at the pH level required for lysine-selective bioconjugation (intrinsic pKa of lysine's ε-amine = 10.4) [17]. However, as the constrained pyrrole-2,5-dione ring significantly promotes hydrolysis; the corresponding acrylamides demonstrate far greater stability under basic aqueous conditions. This difference in stability becomes particularly pronounced in *N*-aryl systems. Surprisingly, despite the impressive reactivity of *N*-phenyl acrylamides towards lysine and cysteine residues, their application has been almost exclusively limited to use as covalent inhibitors for drug development, rather than as a means of introducing tags via bioconjugation [18]. For this reason, 4-[4-(pentafluorosulfanyl)phenyl]-2-propenamide (**5a**) was also investigated as a potential prosthetic group for tagging lysine residues with the -SF$_5$ moiety (Figure 1).

To properly ascertain the influence of the -SF$_5$ groups considerable electron-withdrawing effect on these bioconjugate approaches (σ_p = 0.68), a number of analogous, *para*-substituted *N*-aryl maleimide and acrylamide derivatives were also synthesised and subjected to the same bioconjugate reactions for comparison, namely; OMe (σ_p = −0.27), H (σ_p = 0.00) and CF$_3$ (σ_p = 0.54) [3].

2. Results and Discussion

2.1. Kinetic Studies of N-Aryl Maleimide Stability

N-Aryl maleimides were synthesised from the corresponding anilines over a two-step synthesis. The first synthetic step entailed an acylation of the aniline with maleic anhydride using ether as a solvent to give the corresponding *N*-phenyl maleamic acid in yields of 87–95% [19]. The maleamic acid intermediates were then cyclised via reflux with sodium acetate in a solution of acetic anhydride (Scheme 3) [20]. The resulting maleimides were obtained in yields ranging from 79–93% (Supplementary Tables S1 and S2). Dehydrative cyclisation was also attempted using a Dean–Stark apparatus and toluene as a solvent; however, this approach was found to be far less efficient.
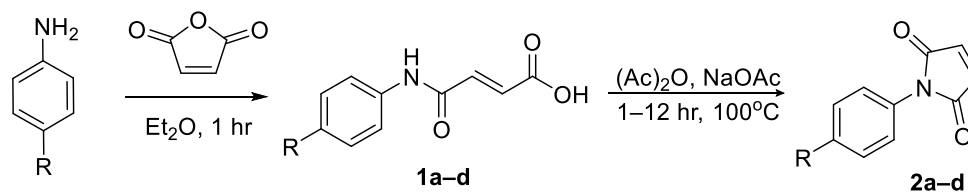
R = SF$_5$ (**a**), CF$_3$ (**b**), H (**c**), OMe (**d**)

Scheme 3. Intermolecular cyclisation of *N*-aryl maleamic acid derivatives into the corresponding *N*-aryl maleimides.

Bioconjugation is almost exclusively performed under partly or entirely aqueous conditions to solubilise hydrophilic target biomolecules such as proteins and preserve their complex secondary or tertiary structures. Therefore, for the maleimide derivatives to be applicable to bioconjugation, they must demonstrate a reasonable degree of aqueous stability. Maleimides are particularly susceptible to hydrolysis relative to other commonly used Michael acceptors, primarily due to the ring strain imposed by the alkene bond.

Although the rate constants for the cysteine–maleimide conjugation reaction are typically orders of magnitude faster than the competing hydrolysis pathway (concentration dependant), minimal degradation of the precursor must occur during sample preparation prior to conjugation to ensure maximal conjugate yield. Additionally, as the thio-succinimide intermediate conjugate is reversible under mildly basic conditions, the maleimide can slowly regenerate and subsequently hydrolyse to the unreactive maleamic acid, resulting in degradation of the thio-succinimide conjugate over time.

Stock 100 mM solutions of the respective maleimides were prepared in anhydrous acetonitrile. These were used to determine the relative rates of hydrolysis across the synthesised maleimide derivatives. These were then automatically injected (10 μL) via HPLC into a secondary sample vial containing a 990 μL solution of 20% MeCN in 50 mM phosphate buffer (pH = 7.4 and 8) to give a final maleimide concentration of 1 mM. This solvent ratio (1:5) and buffer concentration (50 mM) was found to be optimal, as buffer concentrations below 50 mM would be less capable of regulating the pH of the reaction mixture and concentrations above 80 mM phosphate resulted in phase separation between the acetonitrile and buffer due to its ionic strength. Organic buffers such as Tris, TAPS and HEPES, etc., were avoided as they contain nucleophilic groups that can react with the prosthetic groups.

Following the injection of the maleimide stock solution, the reaction mixtures were analysed periodically over 15 min intervals via LC-MS (Figure 2). The hydrolysis reaction was performed at both pH = 7.4 and 8, as the latter is also often used for cysteine–maleimide bioconjugation, particularly where competitive lysine residues are absent or the rate of conjugation must be accelerated.
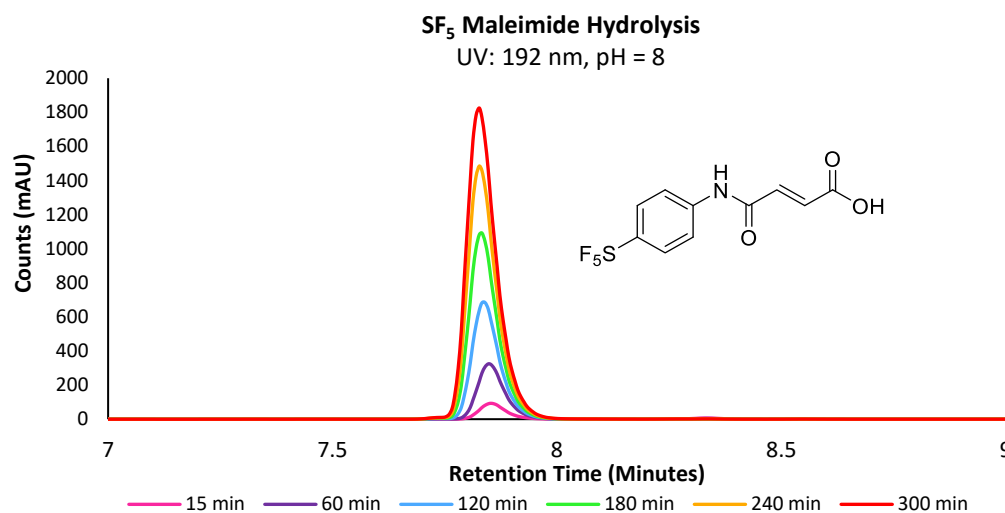
Figure 2. Overlaid UV chromatograms of -SF$_5$ maleamic acid increasing in concentration over the course of 300 min.

A wavelength of 192 nm was found to be optimal for all analytes described herein, due to the common absorption wavelength of their amide bonds. The reported rho reactivity constant (ρ) for maleimide hydrolysis at pH = 8 has been determined in previous studies to be approximately 0.35, indicating that the electrophilicity and ring strain is the primary driving force behind its hydrolytic instability, whereas substituent effects are less significant [21]. However, as the -SF$_5$ group is known to be one of the most electron-withdrawing groups, the evaluation of its influence on hydrolytic stability in comparison with the electron donating -OMe derivative is warranted. As anticipated, maleimide derivatives underwent hydrolysis at higher rates with increasingly electron-withdrawing R substituents, with the -SF$_5$ maleimide undergoing hydrolysis ~6.9 and ~5.6 times faster than the rate of the -OMe derivative at pH = 7.4 and 8, respectively (Supplementary Figures S1 and S2). The comparison is an interesting result, as one might expect the -SF$_5$ group to be more

sensitive to increases in pH than the -OMe derivative, whereas a decrease in the difference of relative rates was observed with increased pH. Similarly, reactions performed at pH = 8 demonstrated a more significant increase in the rate of hydrolysis than when performed at pH = 7.4, with the -SF$_5$ and -OMe derivatives hydrolysing at a 1.4 and 1.8-fold increase in the rate from pH = 7.4, respectively.

2.2. The Maleimide–Cysteine Conjugation

The efficacy of the maleimide–cysteine bioconjugation is heavily dependent on several variables relating to the target biomolecule, particularly the abundance of cysteine residues, the presence of competing residues and the steric accessibility of these residues to the prosthetic group. These variables make it almost impossible to quantitatively assess and compare the efficacy of prosthetic groups between any two biomolecules; for this reason, *N*-acetyl-*L*-cysteine was chosen as a model thiol substrate representative of cysteine residues within proteins and peptides.

The abundance of amino acid residues in a protein with a free terminal α-NH$_2$ is typically very low, as they are tied up in amide or "peptide" bonds between neighbouring amino acid residues. For this reason, the α-NH$_2$ terminus of *L*-cysteine was protected with an acetyl group; protecting the α-amine is also crucial, as it would participate heavily as a competing nucleophile in the analytical-scale reactions described herein. The carboxy terminus was not protected, as the nucleophilic capacity of the carboxylate is greatly diminished by resonance delocalisation of the negative charge. Furthermore, the rate constant for the maleimides reaction with the thiolate anion is orders of magnitude faster. The additional advantage of a free carboxy terminus was that both the *N*-acetyl-*L*-cysteine and conjugates gave powerful signals in ensuing mass spectrometry experiments using a negative ionisation mode.

The initial approach towards synthesising the cysteine–maleimide conjugates was to isolate and purify the thio-succinimide as an external standard for LC-MS investigations. Hence, anhydrous conditions were necessary to avoid hydrolysis of the thio-succinimide into the two corresponding thio-succinamic acid regio-isomers. The reactions were performed in anhydrous acetonitrile using NEt$_3$ as a base. It was found that under these conditions, the reaction proceeded very slowly (>10 h) for all the derivatives. It is suspected that the triethylamine was sufficiently basic to induce the β-elimination of the thio-succinimide, causing the reaction to exist in a constant state of equilibrium and thus never reach completion.

The thio-succinimide derivatives readily underwent hydrolysis during attempts to isolate them, and the subsequent hydrolysis products were challenging to separate using column chromatography, reverse-phase column chromatography or crystallisation. (HRMS spectra for thio-succinimide intermediates 3a–d can be found summarised in Supplementary Table S3). In light of this, the most practical approach was to drive each reaction to its endpoints using aqueous conditions and then isolate the corresponding hydrolysed thio-succinamic regio-isomers (Scheme 4). The information derived from this synthetic approach would also be more powerful, as it would more closely emulate the parameters of a typical bioconjugate reaction with respect to pH and solvent conditions.
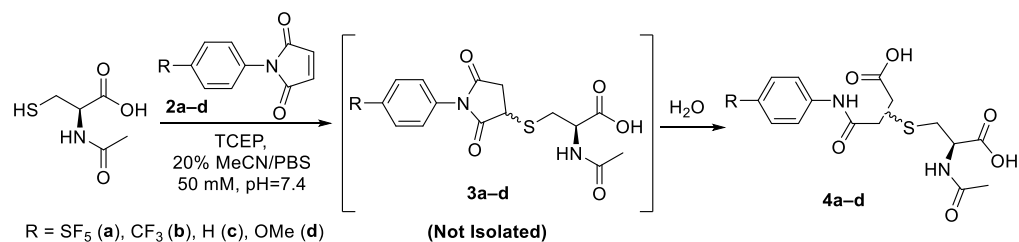
Scheme 4. General synthetic approach for model conjugation of maleimide derivatives with *N*-acetyl-*L*-cysteine.

Except for concentration, reactions were performed under similar conditions to the analytical-scale bioconjugations yet to be described herein. It was found that 20% acetonitrile in 50 mM phosphate buffer (pH = 7.4) was adequate for solubilising both the *N*-acetyl-*L*-cysteine and the *N*-aryl maleimide. The solvent was degassed by bubbling the reaction mixture with nitrogen gas, and then four-equivalents of tris(2-carboxyethyl)phosphine (TCEP) was added to ensure all the thiol was fully reduced and available for the reaction. The reaction was allowed to stir for one hour prior to adding maleimide in anhydrous acetonitrile. Conjugation reactions were allowed to proceed for 12 h. Whereas the formation of the intermediate thio-succinimide was practically instantaneous, the reaction time was extended to ensure they had completely hydrolysed to the final isomeric thio-succinamic acids. The reaction mixtures were then acidified and purified using a C18 reverse-phase preparative cartridge. Yields of the thio-succinamic acids obtained were between 80–96%; no significant correlation can be seen between the electronic properties of the R substituent and yield (Table 1).

Table 1. Yields obtained for thio-succinamic acid conjugates (**4a–d**).

Compound	R	Yield (%)
4a	SF_5	80
4b	CF_3	94
4c	H	96
4d	OMe	92

The reaction rate on a synthetic scale was assessed by adding -SF_5 maleimide (**2a**) into the solution of reduced *N*-acetyl-*L*-cysteine in CD_3OD; the reaction mixture was analysed by ^{1}H-NMR periodically over 5 min increments up to 150 min. Upon addition of the -SF_5 maleimide, the reaction mixture adopted a bright red colour; analysis of the reaction mixture by ^{1}H-NMR immediately after addition revealed that the maleimide had been fully and instantaneously consumed, as evident from the lack of a vinylic CH singlet at ~6.9 ppm (Figure 3). After 12 h, the reaction mixture was analysed again, revealing no change. From both the aromatic region and numerous singlets at ~2 ppm corresponding to the *N*-acetyl -CH_3, it is evident that a variety of conjugate species had formed. This is most likely attributed to the two regio-isomers of the thio-succinamic acids and their two subsequent diastereoisomers arising from the chiral centre at the C-S carbon. Structural elucidation of the regio-isomeric mixture can be seen from COSY and HSQC example spectra (Supplementary Figures S4 and S5 and Table S4). Based on the integration of the *N*-acetyl -CH_3 groups, ^{1}H-NMR analysis of the respective regio-isomeric mixtures would indicate that there is little selectivity for one regio-isomer over the other, each isomer being present in a 50:50 ratio following hydrolysis of the thio-succinimide intermediate.
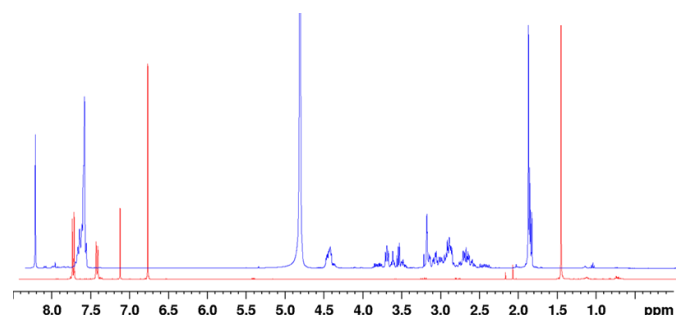
Figure 3. ^{1}H-NMR of the conjugation reaction mixture immediately after adding -SF_5 maleimide (blue) and the pure maleimide precursor (red), indicating the maleimide had been immediately consumed, as indicated by the absence of a vinylic singlet peak at 6.9 ppm. NMR spectra are overlaid on a skewed Z axis.

2.3. Kinetic Studies of the Maleimide–Cysteine Conjugation

The cysteine–maleimide conjugation LC-MS experiments followed a similar protocol to the maleimide hydrolysis study. Maleimides were prepared in a 100 mM stock solution of anhydrous acetonitrile. The maleimide stock solution (10 μL) was automatically transferred into a secondary vial containing a solution of degassed *N*-acetyl-*L*-cysteine (10 mM) and TCEP (40 mM). To preserve pseudo-first-order rate kinetics, the *N*-acetyl-*L*-cysteine was used in ten equivalents relative to the maleimide (1 mM).

The reactive -SF$_5$ maleimide (**2a**) was observed for the initial injection of the conjugation reaction with *N*-acetyl-*L*-cysteine. However, the signal had completely disappeared by the first 15 min time-point (Supplementary Figure S3). All *N*-aryl maleimide derivatives had been consumed within the first 15 min of their respective conjugation reactions. This would indicate that the maleimide had been entirely consumed through either the formation of the corresponding thio-succinimide conjugate or hydrolysis to form the *N*-aryl maleamic acid. Considering the concentration at which the analytical bioconjugation reaction was performed, the -SF$_5$ maleimide qualifies well for the prosthetic group criteria relating to reactivity. Interestingly, despite the lack of visible maleimide, the signal corresponding to the maleamic acid hydrolysis product continued to increase over time. The most likely explanation is that the thio-succinimide was regenerating small amounts of the maleimide via β-elimination and instantaneously hydrolysing to the corresponding *N*-aryl maleamic acid (Supplementary Figure S5).

Figure 4a shows the thio-succinimide at a relatively high concentration from the initial time-point, decreasing over time and then beginning to re-accumulate. In addition to the disappearance of observable maleimide, the initial high concentration of thio-succinimide would also support the notion that the maleimide had completely reacted within the first 15 min. The subsequent decrease in thio-succinimide concentration could most likely be attributed to consumption via the hydrolytic ring opening to the corresponding isomeric thio-succinamic acids (Scheme 5). The absence of the -SF$_5$ maleamic acid at the first time-point indicates that the preparative maleimide purification procedure was effective and that the reaction solvent was sufficiently dry for LC-MS analysis.
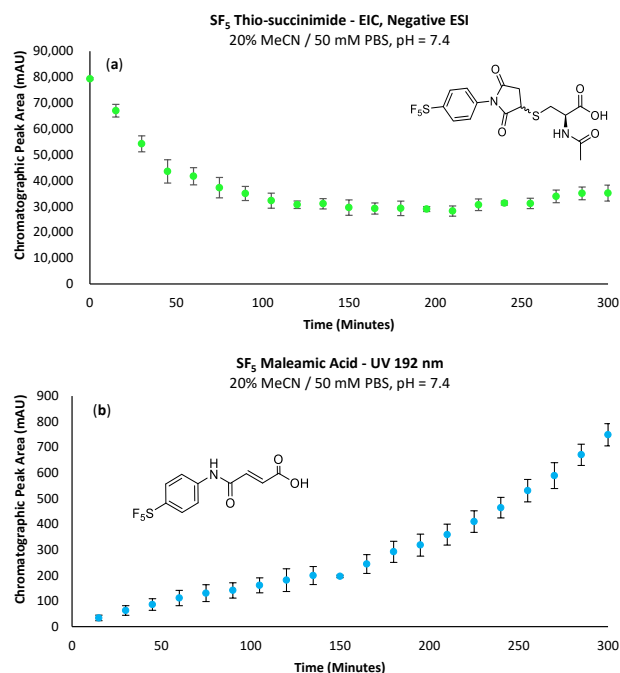
Figure 4. (**a**) Change in EIC peak area corresponding to the -SF$_5$ thio-succinimide intermediate over time; performing the conjugation in triplicate reveals a lower standard deviation relative to the integration of UV chromatograms. (**b**) Accumulating -SF$_5$ maleamic acid (**1a**) via β-elimination of the thio-succinimide intermediate over time.
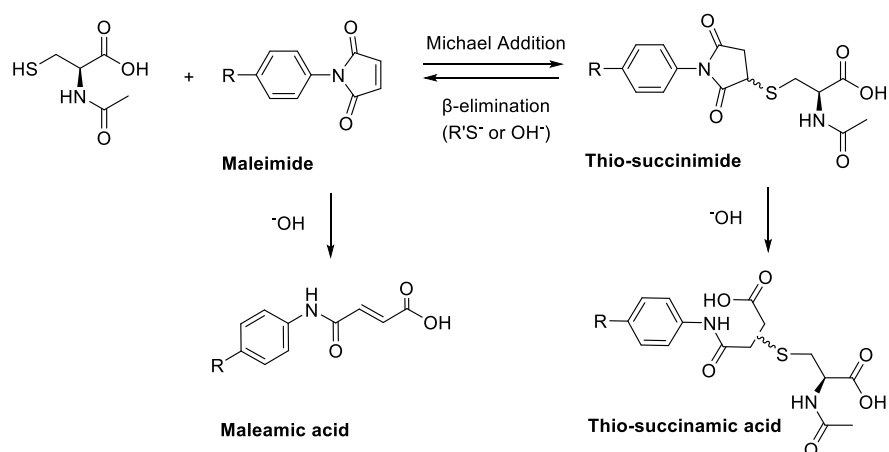
Scheme 5. Reaction pathways of the maleimide–cysteine conjugation.

Although β-elimination is another pathway through which a decrease in thio-succinimide concentration might be observed, the ten equivalents of cysteine and far greater rate constant for the forwards Michael addition reaction would render the β-elimination effectively unobservable. However, the determination of β-elimination can be deduced from the *N*-aryl maleamic acid accumulation rate, as a small proportion of the regenerated maleimide will hydrolyse irreversibly rather than undergo the preferential Michael addition reaction (Figure 4b).

Explanations for the final increase in thio-succinimide concentration are uncertain, as the maleimide appears to be totally consumed early in the reaction and the formation of the thio-succinamic acids is non-reversible. One theory is that as cysteine is consumed in the form of the thio-succinamic acids, less thiolate is available to promote the β-elimination of the thio-succinimide; however, ten equivalents of cysteine are used, so one might expect this change in nucleophile concentration to be negligible.

The higher rate of re-accumulation for the -OMe thio-succinimide (Figure 5) relative to the -SF$_5$ derivative (Figure 4a) is consistent with this theory, as the rate of -SF$_5$ thio-succinimide hydrolysis will be far greater than that of the -OMe derivative due to the electron-withdrawing effect of the -SF$_5$ group increasing the electrophilicity of the carbonyl carbons and thus promoting their attack by hydroxide anions.
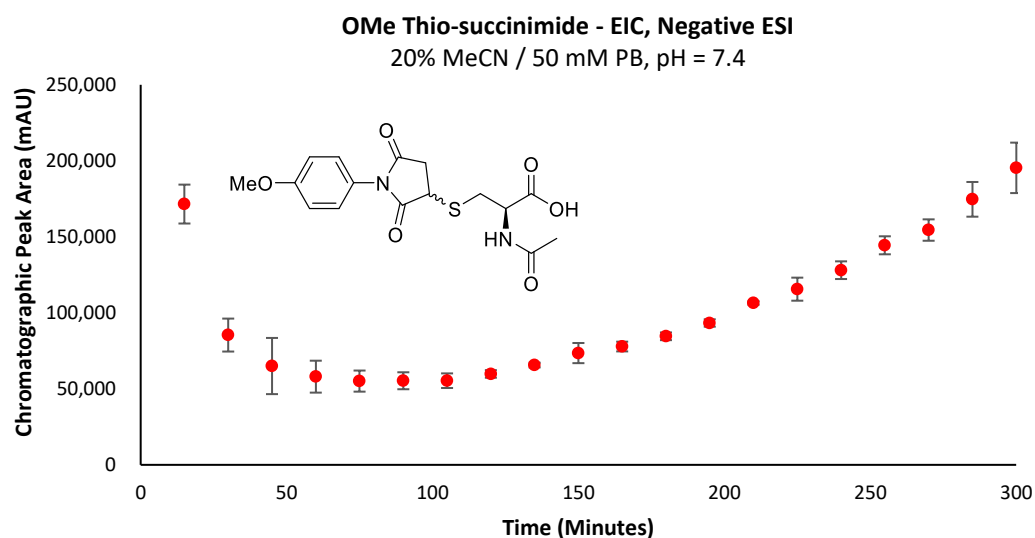
Figure 5. EIC chromatographic peak area corresponding to the -OMe thio-succinimide intermediate over time.

The objective of these analytical experiments was to obtain a rate constant for both thio-succinimide and thio-succinamic acid formation; however, due to the complexity of the reaction regarding β-elimination, and the concurrent ring opening, it is virtually impossible to fit a rate constant to any given reaction. Baldwin et al. and Fontaine et al. successfully quantified these rates in similar experiments using aliphatic maleimide derivatives. However, the *N*-aryl derivatives described in this work are substantially more reactive towards both β-elimination and ring opening, making the isolation of conjugate intermediates unfeasible for use as an external standard [14,15]. Whereas quantitative information concerning the rate constant cannot be extrapolated from this data, relative information regarding the reactivity of *N*-aryl prosthetic groups is still useful.

The relative stabilities of the thio-succinimide intermediates are further reflected in the analysis of the corresponding thio-succinamic acids. The thio-succinamic acid regio-isomers were all separable using the standard LC method (Figure 6). As the distribution of regio-isomers is not overly relevant, the peak area for both isomers was integrated and the data were represented for the mixture.
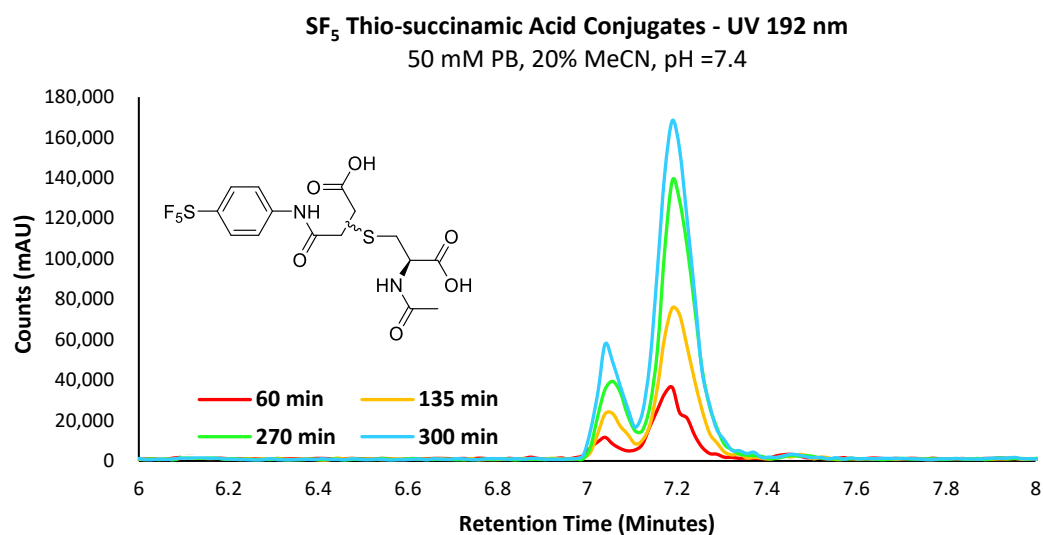
Figure 6. UV chromatogram depicting the increase in the concentration of the -SF$_5$ thio-succinamic acid regio-isomers over 300 min.

The -SF$_5$ thio-succinamic acid is evident from the first time-point (Figure 7a); comparatively, the -OMe derivative does not show a substantial increase in concentration until 120 min into the conjugation reaction (Figure 7b). This supports the decreased hydrolytic stability of the -SF$_5$ thio-succinimide that is attributed to the -SF$_5$ group's strong electron-withdrawing effect. These are promising results regarding using the -SF$_5$ maleimide as a potential prosthetic group, as the hydrolytic instability of the thio-succinimide intermediate limits the conjugates' opportunity to undergo β-elimination or the subsequent thiol exchange with endogenous biomolecules. Data for the formation of **4c** can be found in the Supplementary Information (Supplementary Figure S7).
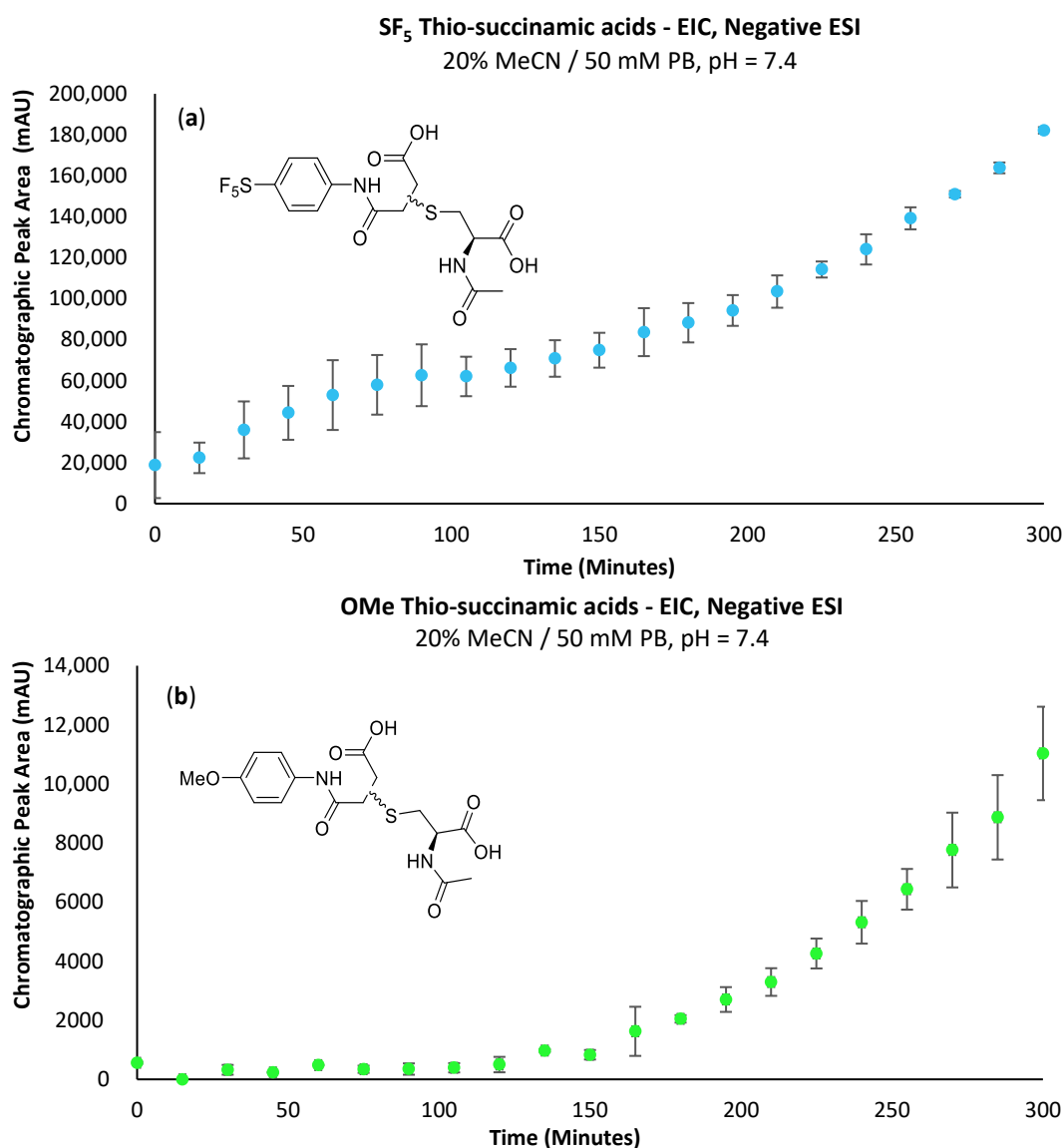
Figure 7. (**a**) Graph depicting the increase in EIC chromatographic peak area of the -SF$_5$ thio-succinamic acid regio-isomers over 300 min. (**b**) Graph depicting the increase in EIC chromatographic peak area of the -OMe thio-succinamic acid regio-isomers over 300 min.

2.4. Application of the Maleimide–Cysteine Conjugation to cRGD Peptide

Cyclic RGD peptides (cRGD) have been utilised extensively in radiochemistry to identify tumours' locations via PET diagnostic imaging. These peptides have an affinity for $\alpha v \beta 3$ receptors on the surface of endothelial cells. $\alpha v \beta 3$ receptors are heavily implicated in angiogenesis. For this reason, these receptors are particularly over-expressed in malignant endothelial cells and on a variety of other tumour cells [22].

Regarding the activity and selectivity of cRGD peptides towards $\alpha v \beta 3$ receptors, their binding affinity is primarily imparted by the arginine (R), glycine (G) and aspartic acid (D) motif (Figure 8) [23]. The fourth position (4: *D*-phenylalanine) has been found to provide the greatest binding affinity when substituted with a *D*-phenylalanine residue. In contrast, the fifth position (5: conjugation point) was found to have little influence on binding affinity and is, therefore, an ideal site for incorporating radiolabels via conjugation with reactive amino acids [24].
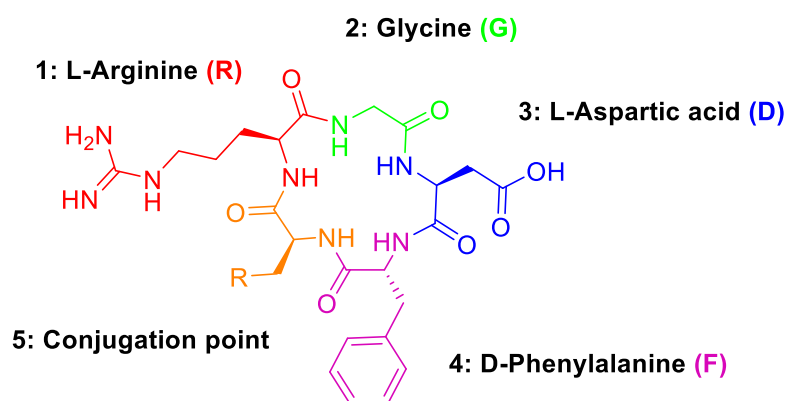
Figure 8. Amino acid groups of cRGD peptides and their structural motifs.

In this case, a cysteine residue was chosen as the fifth amino acid for chemo-selective bioconjugation with the synthesised -SF$_5$ maleimide. The cRGDfK peptide is advantageous as a target for bioconjugation as, being a small peptide, the steric access of the maleimide to the cysteine side chain is relatively unhindered by neighbouring amino acids or more complex secondary or tertiary structures.

Analytical-scale reactions with the cRGD peptide followed the same general procedure as the conjugations performed with *N*-acetyl-*L*-cysteine (Scheme 6). Similarly, the -SF$_5$ maleimide (**2a**) was consumed within the first 15 min of the reaction with cRGDfK. Figure 9a,b almost mirror one another, showing a strong correlation between the consumption of the cRGD thio-succinimide and the formation of the corresponding thio-succinamic acid conjugates. Much like the conjugation performed with *N*-acetyl-*L*-cysteine, the cRGDfK thio-succinimide conjugate hydrolysed rapidly, reaching 50% of its initial concentration after 105 min. Due to the complexity of the cysteine–maleimide conjugation, however, a rate constant cannot be derived from the data.
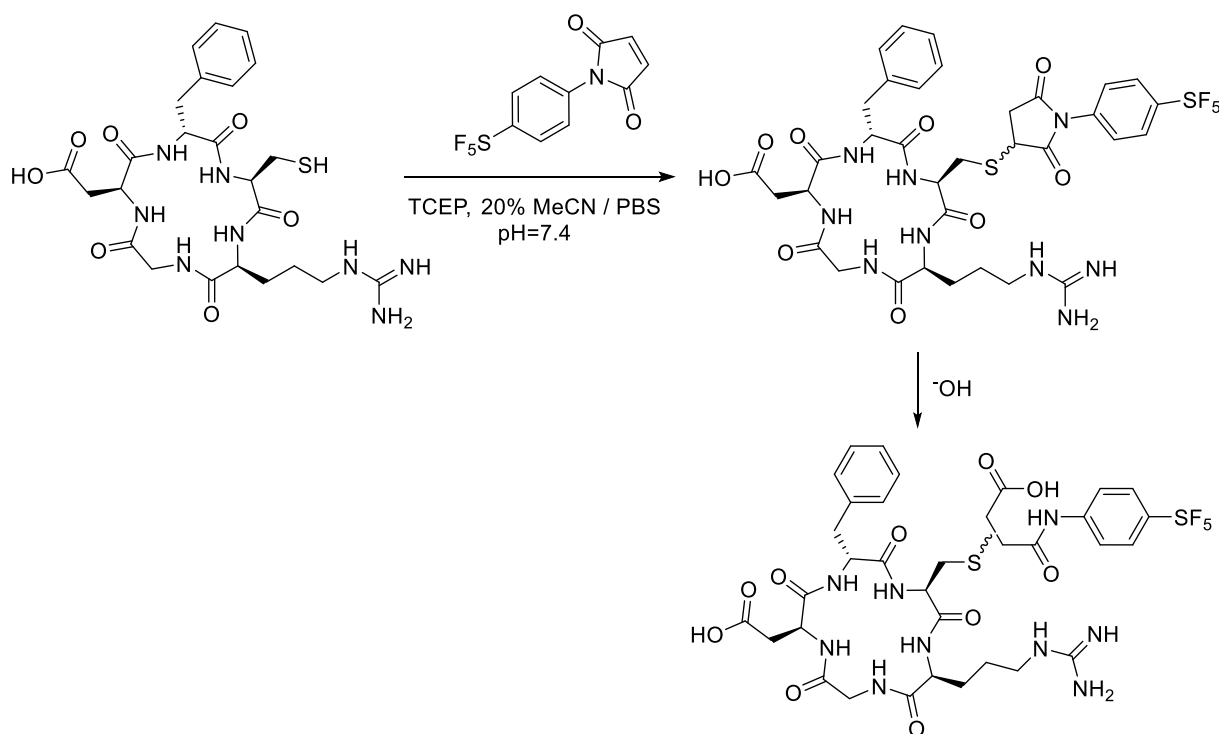
Scheme 6. Analytical-scale bioconjugation of -SF$_5$ maleimide with cRGDfK peptide.

cRGDfK - Thio-succinimide Conjugate - EIC, Negative ESI
20% MeCN / 50 mM PB, pH = 7.4

cRGDfK - Thio-succinamic Acid Conjugate - EIC, Negative ESI
20% MeCN / 50 mM PB, pH = 7.4
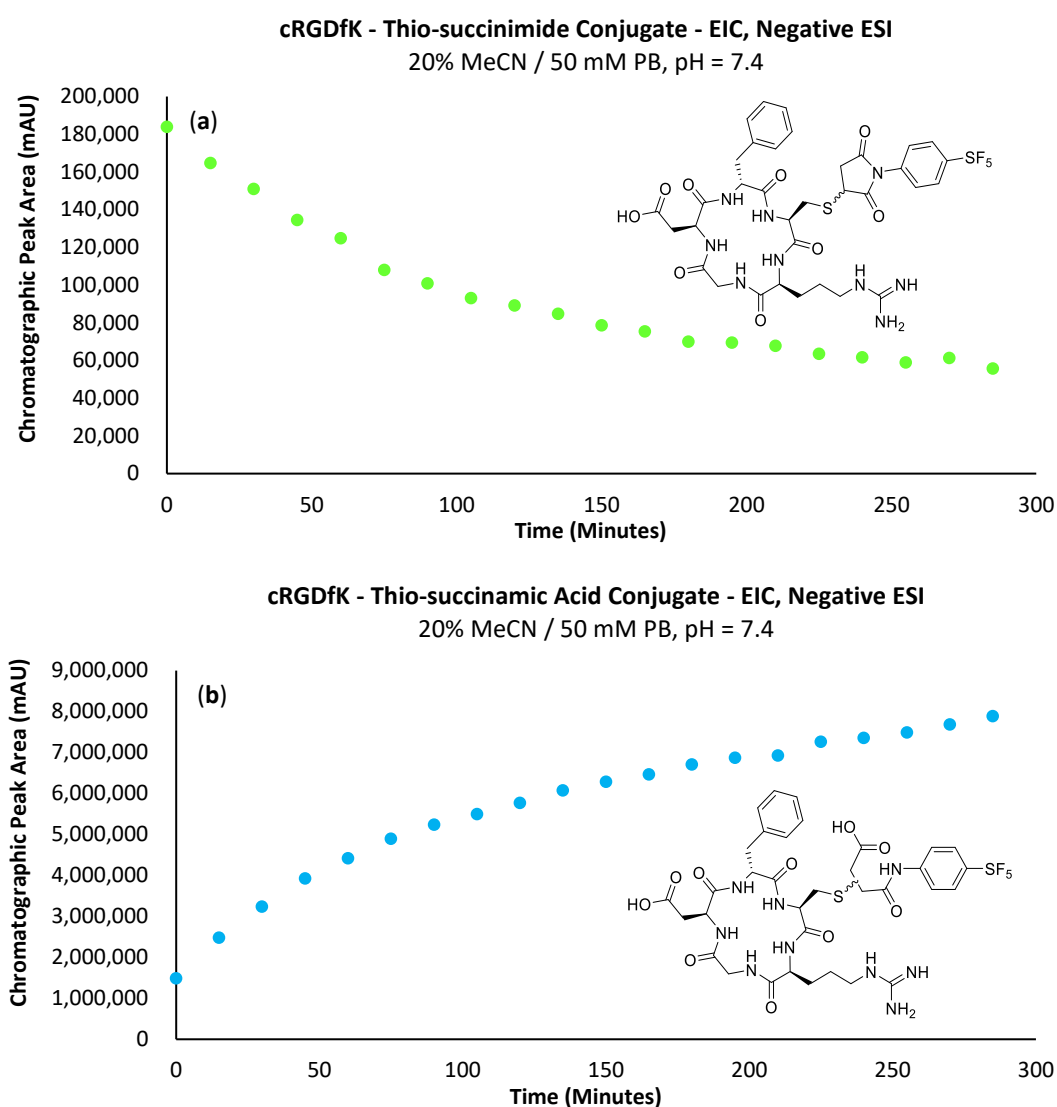
Figure 9. (**a**) Graph depicting the EIC chromatographic peak area increase in the -SF$_5$ maleimide–cRGDfK peptide thio-succinimide conjugate over 300 min. (**b**) Graph depicting the increase in EIC chromatographic peak area of the -SF$_5$ maleimide–cRGD peptide thio-succinamic acid conjugate over 300 min.

Results from the LC-MS experiments indicate the bioconjugation reaction to be successful when up-scaled to a concentration appropriate for bioconjugation. From the analytical bioconjugation reactions performed with cRGDfK and *N*-acetyl-*L*-cysteine, the -SF$_5$ maleimide appears promising for use as an effective prosthetic group for incorporating the -SF$_5$ moiety onto biomolecules of interest. Although the maleimide is unstable under aqueous conditions, the rate of the cysteine conjugation substantially outcompetes the hydrolysis pathway. The added advantage of the -SF$_5$ maleimide is the hydrolytic instability of the thio-succinimide intermediate, which rapidly undergoes hydrolysis in solution to the stable and non-reversible thio-succinamic acid conjugate.

2.5. Synthesis of N-Aryl Acrylamide Derivatives

The approach for the synthesis of *N*-aryl acrylamide derivatives entailed an acylation reaction using acryloyl chloride. Diisopropylethylamine (DIPEA) was used as a non-nucleophilic base and DCM as a solvent (Scheme 7) [25]. The *N*-phenyl acrylamide derivatives were obtained in yields ranging between 69 and 81% (Supplementary Table S5).
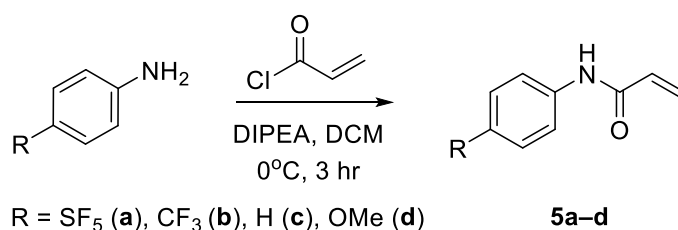
Scheme 7. Synthesis of *N*-aryl acrylamides via acylation of the corresponding anilines.

2.6. Kinetic Studies of N-Aryl Acrylamide Stabilities

The relative rates of hydroxylation across the various acrylamide derivatives synthesised were determined to assess the applicability of the -SF$_5$ acrylamide as a prosthetic group. Acrylamide 100 mM stock solutions were prepared in anhydrous acetonitrile. Each solution was automatically injected (10 µL) via HPLC into a secondary sample vial containing a 990 µL solution of 20% MeCN in 50 mM phosphate buffer (pH 8) to give a final acrylamide concentration of 1 mM.

The hydroxylation reaction was performed at pH = 8, a typical pH for targeting lysine residues. Of course, if competing cysteine residues are present, the conjugation can be performed at a higher pH to improve selectivity towards lysine, at the risk of degrading the target biomolecule. Following the injection of the acrylamide stock solution, the reaction mixtures were analysed periodically over 15 min intervals via LC-MS. Unlike the maleimide hydrolysis study, the acrylamides were easily ionised using a negative ionisation mode and absorbed strongly at 192 and 273 nm wavelengths.

The initial objective of this study was to analyse the decrease in acrylamide concentration over time; however, the -SF$_5$ acrylamide concentration was inexplicably found to increase linearly, and this was observed consistently over multiple repeats. (Supplementary Figure S7). Hydrolysis experiments performed with corresponding -H, -OMe and -CF$_3$ acrylamides all gave the same unprecedented increase in acrylamide concentration over time. This increase in acrylamide concentration was most likely attributed to the poor solubility of *N*-aryl acrylamides in aqueous media. In an effort to completely solubilise the acrylamide within the reaction mixture, the proportion of acetonitrile co-solvent was increased from 20 to 30% *v/v*, the volume of acrylamide stock solution transferred to the reaction vial was also decreased from 10 to 1 µL, giving a final acrylamide concentration of 0.1 mM. However, these adjustments did not change the outcome, and the acrylamide concentration continued to increase over time.

As the issue relating to the increase in acrylamide concentration was not resolved, the corresponding hydroxylation product was analysed instead to at least provide some indication of aqueous stability. The primary aqueous degradation product of the acrylamide would naturally be expected to be the corresponding alcohol, arising via the nucleophilic attack of the acrylamide by the hydroxide anion (Figure 10).

No trace of the primary alcohol hydroxylation products was observed for any of the -CF$_3$, -H or -OMe derivatives by UV or mass detectors, indicating that only the -SF$_5$ acrylamide was reactive enough to undergo any measurable hydroxylation within the five hours following injection. From this data, it is evident that the rate of hydroxylation for the acrylamide derivative was very slow, especially relative to the corresponding maleimide derivatives and would therefore be suitable for use in a further investigation as a potential prosthetic group for incorporating the -SF$_5$ moiety.
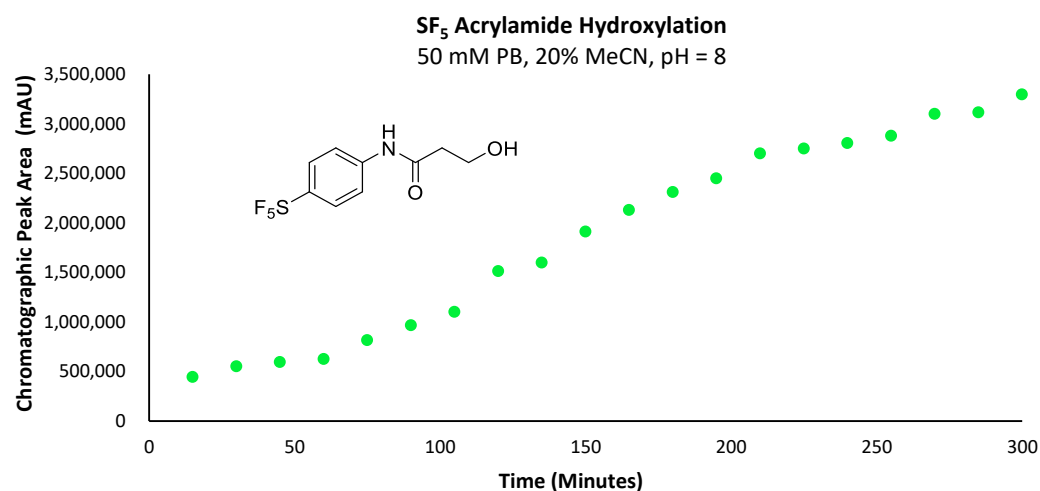
Figure 10. Graph depicting the increase in total chromatographic peak area corresponding to the -SF$_5$ acrylamide hydroxylation product over the course of 300 min.

2.7. Acrylamide–Lysine Conjugation

The acrylamide–lysine conjugations were first attempted using the standard 20% MeCN in phosphate buffer (50 mM, pH = 10) solvent system; however, it was found that the -SF$_5$ acrylamide exhibited poor solubility under aqueous conditions, which was primarily attributed to the lipophilicity of the -SF$_5$ group. A variety of aqueous solvent systems were prepared in an attempt to find an optimal solvent system capable of solubilising the -SF$_5$ acrylamide; it was found that even 40% (*v/v*) concentrations of organic co-solvents, including dimethyl formamide (DMF) and dimethyl sulfoxide (DMSO), were incapable of fully solubilising the acrylamide at 0.025 mmol concentrations (Supplementary Table S6).

The inclusion of water in the reaction mixture was desirable, as it has been suggested to discourage di-alkylation of the conjugate product and promote the reaction through hydrogen bonding interactions [26]. As the lipophilicity of the -SF$_5$ acrylamide did not allow for its solubilisation in water/organic co-solvent mixtures on a synthetic scale, water was omitted from the reaction mixture entirely. Anhydrous acetonitrile was also not capable of solubilising the N_α-acetyl-*L*-lysine precursor. It was reasoned that methanol would provide the desired hydrogen bonding interactions to promote the reaction and fully solubilise all components in the reaction mixture. The aza-Michael addition reaction with N_α-acetyl-*L*-lysine's ε-amine would greatly out-compete any potential side reaction arising from nucleophilic attack by methanol, assuming the reaction mixture was sufficiently basic.

Initially, triethylamine (NEt$_3$) was used as a non-nucleophilic base to deprotonate the lysine substrate. However, this proved detrimental to the reaction as it induced the β-elimination of the conjugate product. When the reaction was allowed to proceed for over 18 h in methanol, the acrylamide substrate was still evident by ^{1}H-NMR, despite using 1.5 stoichiometric equivalents of N_α-acetyl-*L*-lysine. This indicates that the acrylamide precursor was perpetually regenerated via β-elimination of the conjugate product through basic abstraction of the α-proton by NEt$_3$. When anhydrous sodium carbonate was used as a milder base, ^{1}H-NMR indicated the acrylamide had been completely consumed after one hour, with no evidence of β-elimination.

After optimising the reaction conditions (Scheme 8), the conjugation reactions were performed with the other *para*-substituted acrylamide derivatives. Reactions were performed on a 0.2 mmol scale in methanol (1 mL) to emulate the best reaction conditions that would be used for bioconjugation. After one hour, the solutions were acidified and then purified using C18 preparative cartridges. The corresponding lysine–acrylamide conjugates were obtained in modest to high yields (58–89%) (Table 2). Interestingly, when the crude reaction mixtures were analysed by LC-MS, only a minuscule amount of di-alkylation had

occurred, most likely prevented by steric hindrance; a promising result considering the high concentration of the reaction mixture (Supplementary Figure S8).

R = SF$_5$ (**a**), CF$_3$ (**b**), H (**c**), OMe (**d**)
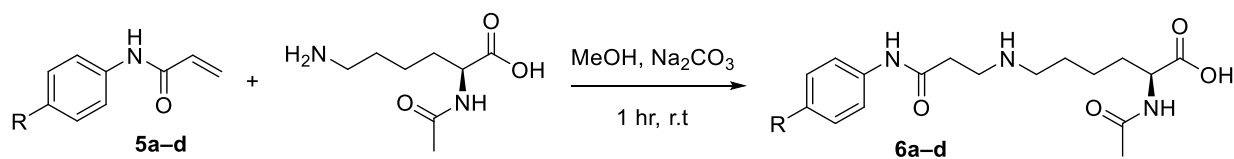
Scheme 8. Optimised reaction conditions for the model lysine–acrylamide conjugation.

Table 2. Yields obtained of the lysine–acrylamide conjugates (**6a–d**).

Compound	R	Yield (%)
6a	SF$_5$	83
6b	CF$_3$	89
6c	H	64
6d	OMe	58

As the synthesised acrylamides were found to be successful on a synthetic scale regarding reaction rate and conjugate yield, the relative reactivities of the acrylamide derivatives were then assessed using the standard LC-MS procedure developed for monitoring the reaction rate of maleimides. In an effort to preserve pseudo-first-order rate kinetics, the N_α-acetyl-*L*-lysine was used in 10 equivalents relative to the acrylamide derivatives. The primary variation to the LC-MS protocol used for the maleimide conjugation study was investigating a broader pH range (pH 7.4–10). The pH used for bioconjugation must be chosen carefully, as several side reactions might occur, such as conjugation with non-targeted residues or degradation of the biological substrate. For this reason, the aza-Michael addition reaction was performed at pH = 7.4, 8 and 10 to assess its influence on the reaction rate.

Analysis of the obtained data revealed that the reaction rate increases with pH (Figures 11 and 12a,b). At a pH of 7.4, very little of the lysine substrate is available for reaction (approximately 0.1%). However, as the reaction proceeds, the basicity of the conjugate preferentially abstracts protons from the lysine precursor, driving the reaction forwards; hence, we still see a marginally increased reaction rate with the electron-deficient acrylamides. However, at pH 8, the slope of the curve for both the -SF$_5$ and -CF$_3$ acrylamide derivatives is substantially steeper relative to the more electron-rich -OMe derivative. This indicates that the influence of acrylamide electrophilicity is becoming more pronounced and is no longer solely reliant on the abundance and nucleophilicity of the ε-amine substrate. As the pH approaches the pKa of the ε-amine (i.e., pH = 10), the basicity of the conjugate is no longer the significant driving force perpetuating the reaction; instead, its rate is primarily influenced by the electrophilicity of the acrylamide. The chromatographic plot for the formation of 6c can be found in the Supplementary Materials section (Supplementary Figure S9).
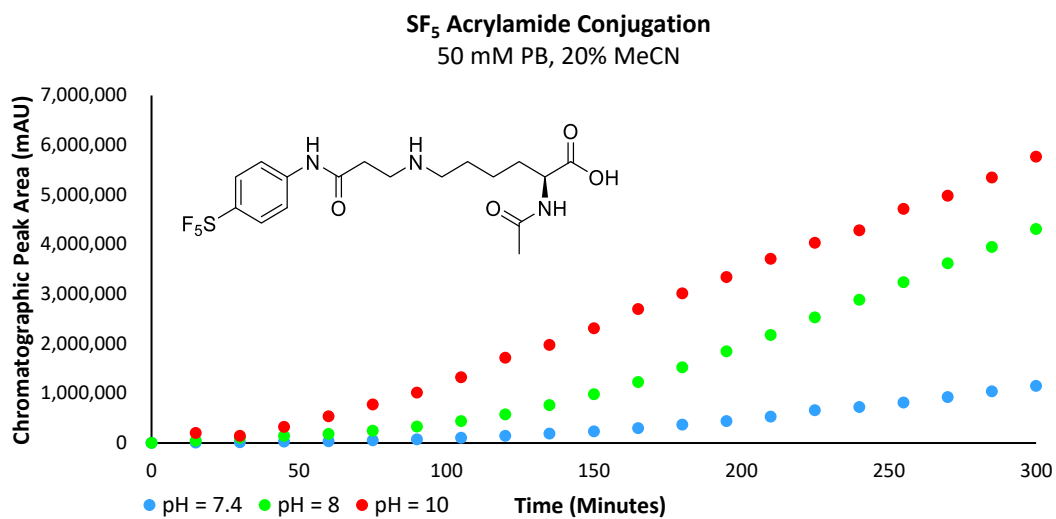
Figure 11. Graph plotting chromatographic peak area corresponding to the -SF$_5$ acrylamide conjugate.
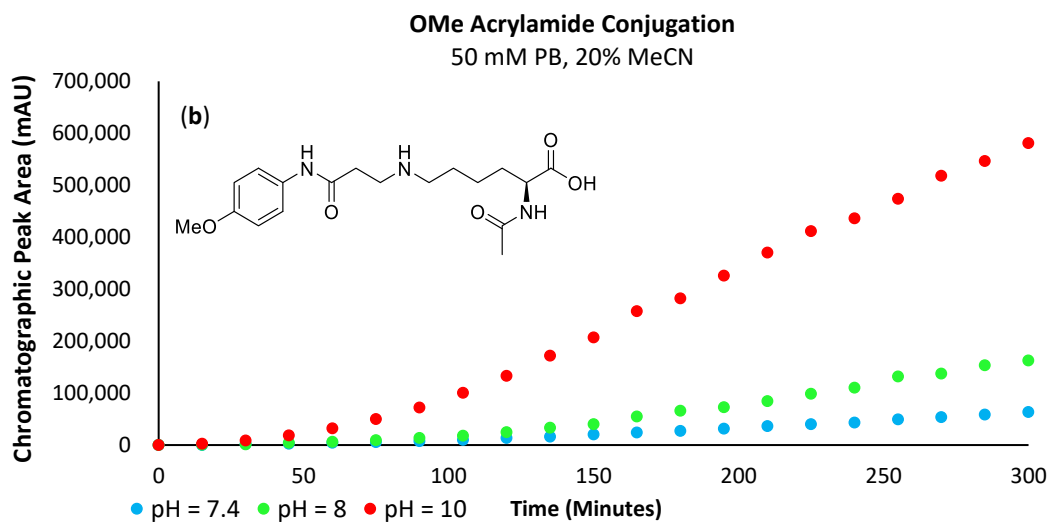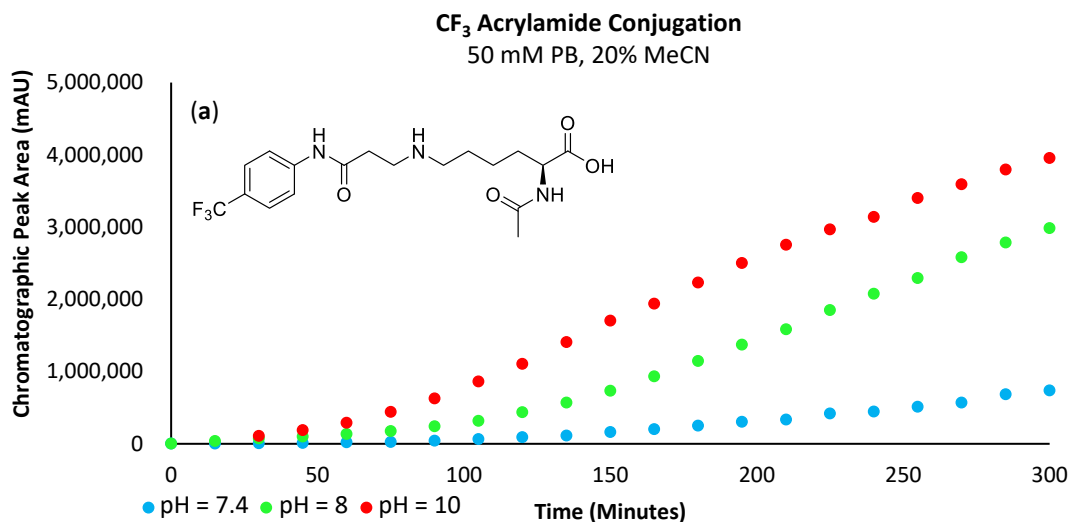
Figure 12. (**a**) Graph plotting chromatographic peak area corresponding to the -CF$_3$ acrylamide conjugate. (**b**) Graph plotting chromatographic peak area corresponding to the -OMe acrylamide conjugate.

2.8. Application of the Acrylamide–Lysine Conjugation to cRGD Peptide

To account for the limited solubility of **6a** in aqueous media, the proportion of acetonitrile in the reaction mixture for the conjugation with cRGDfK was increased to 50% (Scheme 9). Unfortunately, even with a solution of 50% acetonitrile in phosphate buffer (*v/v*), the acrylamide did not appear to solubilise completely; much like the model N_α-acetyl-*L*-lysine, the concentration of the acrylamide increased over time, suggesting the acrylamide was slowly partitioning into the reaction mixture (Supplementary Figure S10). Curiously, the acrylamide's increase in concentration is very linear (R = 0.9952); typically, the rate of dissolution decreases over time as the solution becomes increasingly saturated. Additionally, the acrylamide is rapidly consumed upon dissolution to form the cRGD conjugate, which would be expected to further reduce the linearity of the curve (Supplementary Figure S11).
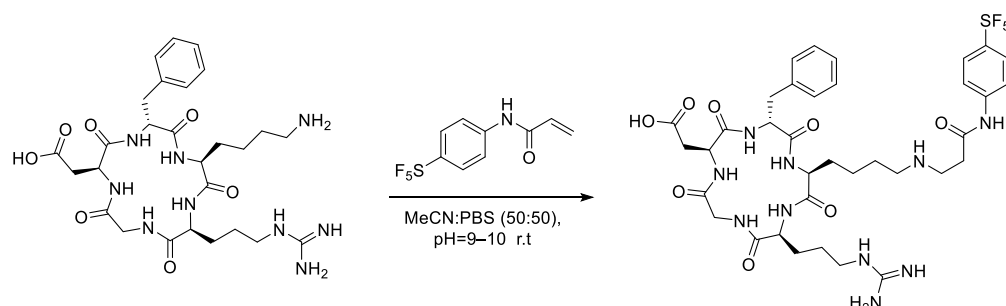
Scheme 9. Reaction conditions utilised for the LC-MS-scale conjugation reaction between -SF$_5$ acrylamide and cRGDfK peptide.

Nevertheless, the acrylamide was still capable of partitioning into the solvent over time, particularly as solvated acrylamide is consumed in the conjugation reaction. However, the dissolution rate will substantially alter the conjugation rate, as indicated by the lack of linearity in the curve of Figure 13 for a reaction designed to demonstrate pseudo-first-order rate kinetics. One positive result from this experiment was that no by-product formation was observed relating to side reactions occurring with the arginine or aspartic acid residues, even at a pH of 8, where the amine is partially protonated. Additionally, no di-alkylation of the conjugate secondary amine substrate was observed.
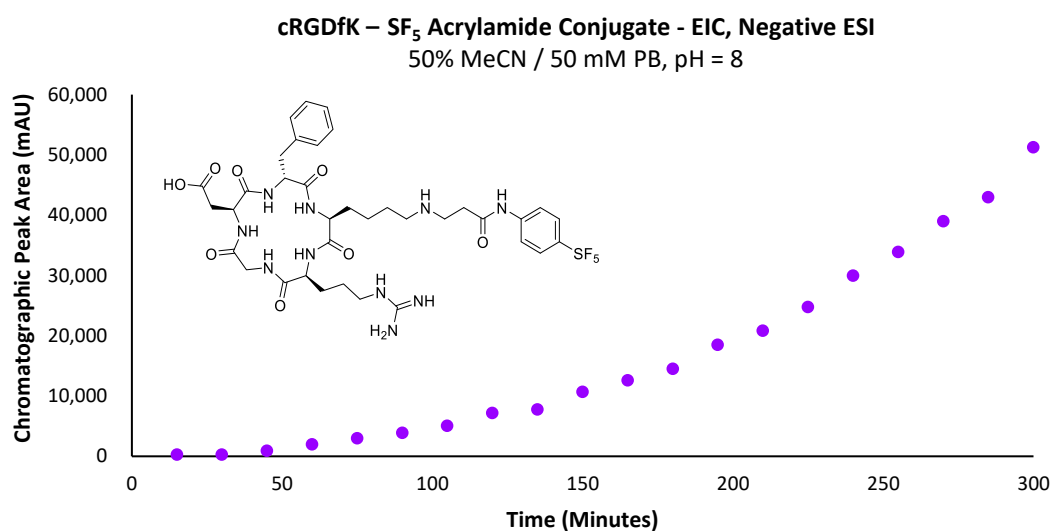
Figure 13. Graph depicting the increase in total chromatographic peak area corresponding to the -SF$_5$ acrylamide–cRGDfK peptide conjugate over time.

3. Materials and Methods

General Experimental: All chemical reagents and AR grade or analytical grade solvents were acquired from commercial sources; 4-(pentafluorosulfanyl) aniline was purchased from Fluorochem and all other compounds were purchased from Sigma-Aldrich Merck unless otherwise stated. All reactions were monitored using TLC Silica gel 60 F_{254} with UV detection at 254 nm. Solvents were removed under reduced pressure using a Buchi rotary evaporator. High-resolution mass spectra were obtained using an Agilent 6510 Q-TOF Mass Spectrometer (ESI) and Agilent 1290 Infinity HPLC system. IR spectra were recorded on a Nicolet 6700 FT-IR spectrometer (KBr). Data for IR were recorded as follows: wavelength (cm^{-1}), absorbance (s = strong, m = medium, w = weak, br = broad). ^{1}H-NMR, ^{13}C-NMR and ^{19}F-NMR spectra were recorded on a Bruker Ascend premium shielded spectrometer 400 MHz (400 MHz ^{1}H, 125 MHz ^{13}C, 376 MHz ^{19}F). Data for ^{1}H, ^{19}F and ^{13}C NMR were recorded as follows: chemical shift (δ, ppm), multiplicity (s = singlet, d = doublet, t = triplet, q = quartet, m = multiplet, br = broad).

General LC-MS method: Reactive prosthetic groups were prepared in a 100 mM stock solution of anhydrous acetonitrile. The stock solution (10 μL) was automatically transferred into a secondary vial containing a degassed solution of the relevant buffer (800 μL), acetonitrile (190 μL) of the model amino acid (10 mM) in the respective buffer solution. The reaction mixture was then mixed 20 times using the auto-injector, and the reaction was analysed by LC-MS periodically every 15 min. In experiments investigating cysteine conjugations, amino acid reaction solutions were incubated with TCEP (4 equiv.) for two hours before injecting the prosthetic group stock solution.

Mass spectrometry parameters: negative ESI, gas temperature 350 °C, drying gas 13 L/min, nebuliser 55 psig, capillary voltage 3500 V, fragmentation voltage 100 V. Mobile phase: solvent A: acetonitrile (0.1% TFA), solvent B: Milli-Q water (0.1% TFA); Mobile phase gradient: 2 min 95% A; 10 min 5% A, 12 min 5% A, 15 min 95% A. Flow rate 0.5 mL/min. Injection volume 10 μL. An injector program achieved the automatic transfer of prosthetic group stock solution to reaction vials. Separation was achieved using a Kinetex 2.6 μm XB-C18 column 50 × 4.6 mm.

Procedures and spectral data for the synthesis of **1a–d**, **2a–d** and **5a–d** can be found in the Supplementary Information.

General procedure for the synthesis of (**4a–d**): *N*-acetyl-*L*-cysteine (32 mg, 0.2 mmol) and TCEP·HCl (115 mg, 0.4 mmol, 2 equiv.) were dissolved in a degassed solution of methanol (2 mL) and sodium carbonate (128 mg, 1.2 mmol, 6 equiv.) and the solution was allowed to stir for 30 min. N-aryl maleimide (0.3 mmol, 1.5 equiv) was added portion-wise to the solution, and the reaction was allowed to continue for 5 h. The reaction mixture was then concentrated in vacuo, and the resulting residue was suspended in 0.1 M HCl (5 mL) and filtered. The precipitate was then purified on C18 silica to afford the final regio-isomeric mixture of thio-succinamic acid product.

General procedure for the synthesis of (**6a–d**): N_α-acetyl-*L*-lysine (38 mg, 0.2 mmol) was dissolved in a solution of methanol (2 mL) and sodium carbonate (128 mg, 1.2 mmol, 6 equiv.), and the solution was allowed to stir for 30 min. Acrylamide (0.2 mmol) was added portion-wise to the solution, and the reaction continued for 8 h. The reaction mixture was then concentrated in vacuo. The crude residue was purified on C18 silica to afford the final product as the sodium carboxylate salt.

3.1. 2-[[(2S)-2-(Acetylamino)-2-carboxyethyl]thio]-4-[(4-pentafluorosulfanylphenyl)amino]-4-oxobutanoic acid (B) & 3-[[(2S)-2-(acetylamino)-2-carboxyethyl]thio]-4-[(4-pentafluorosulfanylphenyl)amino]-4-oxobutanoic Acid (A)

Compound **4a** was obtained as a transparent oil (77 mg, 0.16 mmol, 80%). HRMS (EI) Calcd for $C_{15}H_{16}F_5N_2O_6S_2$ [M-H]$^-$ 479.0369, [M-H]$^-$ Found 479.0372; IR (KBr): 3326, 3206, 2934, 1703, 1597, 1539, 1405, 1373, 1317, 1256, 1230, 1192, 1107, 968, 831 cm^{-1}; ^{1}H-NMR ((CD$_3$)$_2$CO): δ 7.85–7.82 (m, 4H, Ar), 7.79–7.63 (d, 4H, Ar), 4.82–4.74 (m, 2H, CH-S), 3.92–3.88 (m, 2H, CH-N), 3.35–3.25 (m, 2H, CH$_2$-COOH), 3.17–3.04 (m, 4H, CH$_2$-COOH/CH$_2$-S),

2.89–2.81 (m, 2H, CH$_2$-S), 2.03 (s, 3H, CH$_3$), 2.01 (s, 3H, CH$_3$); ^{13}C-NMR ((CD$_3$)$_2$CO): δ 173.26 (C=O), 173.18 (C=O), 171.95 (C=O), 171.90 (C=O), 171.87 (C=O), 171.39 (C=O), 169.96 (C=O), 169.85 (C=O), 148.85 (quin, J = 17 Hz, SF$_5$) 142.92 (Ar-NH), 142.88 (Ar-NH), 127.59 (quin, J = 4 Hz, SF$_5$), 127.59 (Ar-SF$_5$), 127.55 (Ar-SF$_5$), 119.54 (Ar), 119.46 (Ar), 52.81 (CH-S), 52.51 (CH-S), 42.94 (CH-NH), 42.41 (CH-NH), 39.74 (CH$_2$-S), 39.20 (CH$_2$-S), 34.15 (CH$_2$-COOH), 33.97 (CH$_2$-COOH), 22.57 (CH$_3$); ^{19}F-NMR ((CD$_3$)$_2$CO): δ 85.75 (m, 1F), 63.08 (d, J = 150 HZ, 4F).

3.2. 2-[[(2S)-2-(Acetylamino)-2-carboxyethyl]thio]-4-[(4-trifluoromethylphenyl)amino]-4-oxobutanoic acid (B) & 3-[[(2S)-2-(acetylamino)-2-carboxyethyl]thio]-4-[(4-trifluoromethylphenyl)amino]-4-oxobutanoic Acid (A)

Compound **4b** was obtained as a transparent oil (79 mg, 0.18 mmol, 94%). HRMS (EI) Calcd for C$_{16}$H$_{16}$F$_3$N$_2$O$_6$S [M-H]$^-$ 421.0681, [M-H]$^-$ Found 421.0684; IR (KBr): 3325, 3213, 3123, 2934, 1716, 1607, 1540, 1411, 1374, 1306, 1258, 1164, 1114, 1067, 1016, 969, 842 cm^{-1}; ^{1}H-NMR ((CD$_3$)$_2$CO): δ 7.87–7.83 (m, 4H, Ar), 7.62–7.60 (m, 4H, Ar), 4.82–4.75 (m, 2H, CH-S), 3.93–3.88 (m, 2H, CH-N), 3.35–3.25 (m, 2H, CH$_2$-COOH), 3.15–3.06 (m, 4H, CH$_2$-COOH/CH$_2$-S), 2.87–2.83 (m, 2H, CH$_2$-S), 2.02 (s, 3H, CH$_3$), 2.00 (s, 3H, CH$_3$); ^{13}C-NMR ((CD$_3$)$_2$CO): δ 173.24 (C=O), 173.15 (C=O), 171.91 (C=O), 171.86 (C=O), 169.84 (C=O), 169.72 (C=O), 143.29 (Ar-NH), 143.25 (Ar-NH), 129.39 (Ar-CF$_3$), 126.77 (q, J = 5 Hz, CF$_3$), 125.44 (Ar-CF$_3$), 125.39 (Ar), 125.12 (Ar), 53.17 (CH-S), 52.82 (CH-S), 43.00 (CH-NH), 42.47 (CH-NH), 39.76 (CH$_2$-S), 39.20 (CH$_2$-S), 34.15 (CH$_2$-COOH), 33.96 (CH$_2$-COOH), 22.54 (CH$_3$); ^{19}F-NMR ((CD$_3$)$_2$CO): δ -62.36 (s, 3F), -62.39 (s, 3F).

3.3. 2-[[(2S)-2-(Acetylamino)-2-carboxyethyl]thio]-4-[(phenyl)amino]-4-oxobutanoic acid (B) & 3-[[(2S)-2-(acetylamino)-2-carboxyethyl]thio]-4-[(phenyl)amino]-4-oxobutanoic Acid (A)

Compound **4c** was obtained as a transparent oil (68 mg, 0.19 mmol, 96%). HRMS (EI) Calcd for C$_{15}$H$_{17}$N$_2$O$_6$S [M-H]$^-$ 353.0807, [M-H]$^-$ Found 353.0810; IR (KBr): 3322, 3289, 3079, 1716, 1620, 1597, 1551, 1521, 1445, 1374, 1340, 1317, 1261, 1232m 1177, 1083, 1048, 1000, 915, 869, 811, 754, 738, 688 cm^{-1}; ^{1}H-NMR ((CD$_3$)$_2$CO): δ 7.63 (t, J = 12.4 Hz, 4H, Ar), 7.30–7.25 (m, 4H, Ar), 7.06–7.01 (m, 2H, Ar), 4.84–4.73 (m, 2H, CH-S), 3.92–3.87 (m, 2H, CH-N), 3.33–3.24 (m, 2H, CH$_2$-COOH), 3.17–2.99 (m, 4H, CH$_2$-COOH/CH$_2$-S), 2.83–2.75 (m, 2H, CH$_2$-S), 2.01 (s, 3H, CH$_3$), 1.99 (s, 3H, CH$_3$). ^{13}C-NMR ((CD$_3$)$_2$CO): δ 173.36 (C=O), 173.26 (C=O), 171.99 (C=O), 171.16 (C=O), 169.31 (C=O), 169.22 (C=O), 169.19 (C=O), 169.10 (C=O), 139.96 (Ar-NH), 139.89 (Ar-NH), 139.87 (Ar), 139.80 (Ar), 129.48 (Ar), 124.29 (Ar), 124.21 (Ar), 120.20 (Ar), 53.22 (CH-S), 43.24 (CH-NH), 42.77 (CH-NH), 39.70 (CH$_2$-S), 39.65 (CH$_2$-S), 39.10 (CH$_2$-COOH), 39.05 (CH$_2$-COOH), 22.63 (CH$_3$), 22.59 (CH$_3$).

3.4. 2-[[(2S)-2-(Acetylamino)-2-carboxyethyl]thio]-4-[(4-methoxyphenyl)amino]-4-oxobutanoic acid (B) & 3-[[(2S)-2-(acetylamino)-2-carboxyethyl]thio]-4-[(4-methoxyphenyl)amino]-4-oxobutanoic Acid (A)

Compound **4d** was obtained as a transparent oil (71 mg, 0.18 mmol, 92%). HRMS (EI) Calcd for C$_{16}$H$_{19}$N$_2$O$_7$S [M-H]$^-$ 383.0913, [M-H]$^-$ Found 383.0912; IR (KBr): 3308, 3079, 2935, 2838, 1716, 1651, 1541, 1521, 1464, 1415, 1374, 1301, 1241, 1178, 1029, 969, 830 cm^{-1}; ^{1}H-NMR ((CD$_3$)$_2$CO): δ 7.55–7.52 (m, 4H, Ar), 6.86–6.83 (m, 4H, Ar), 4.84–4.72 (m, 2H, CH-S), 3.92–3.86 (m, 2H, CH-N), 3.75 (s, 3H, O-CH$_3$), 3.74 (s, 3H, O-CH$_3$), 3.29–3.23 (m, 2H, CH$_2$-COOH), 3.17–2.96 (m, 4H, CH$_2$-COOH/CH$_2$-S), 2.80–2.72 (m, 2H, CH$_2$-S), 2.02 (s, 3H, CH$_3$), 1.99 (s, 3H, CH$_3$): ^{13}C-NMR ((CD$_3$)$_2$CO): δ 173.40 (C=O), 173.29 (C=O), 171.96 (C=O), 171.32 (C=O), 171.24 (C=O), 168.86 (C=O), 168.82 (C=O), 168.72 (C=O), 156.85 (Ar-OCH$_3$), 156.79 (Ar-OCH$_3$), 132.95 (Ar-NH), 132.87 (Ar-NH), 121.89 (Ar), 121.79 (Ar), 121.76 (Ar), 121.66 (Ar), 55.59 (O-CH$_3$), 53.14 (CH-S), 52.87 (CH-S), 43.36 (CH-NH), 42.92 (CH-NH), 39.45 (CH$_2$-S), 38.84 (CH$_2$-S), 34.19 (CH$_2$-COOH), 34.05 (CH$_2$-COOH), 22.58 (CH$_3$).

3.5. 2-[[(2S)-2-(Acetylamino)-6-((2-carboxyethyl)amino)-[(4-pentafluorosulfanylphenyl)amino]-4-hexanoic Acid (6a)

Compound **6a** was obtained as a transparent oil (76 mg, 0.166 mmol, 83%). HRMS (EI) Calcd for C$_{17}$H$_{23}$F$_5$N$_3$O$_4$S [M-H]$^-$ 460.1329, [M-H]$^-$ Found 460.1329; IR (KBr): 3263, 2932, 1693, 1625, 1503, 1438, 1399, 1314, 1260, 1188, 1100, 1033, 812, 649, 578, 541, 493 cm^{-1};

^{1}H-NMR (D$_2$O): δ 7.72 (d, J = 8 Hz, 2H, Ar), 7.52 (d, J = 8.4 Hz, 2H, Ar), 4.07 (dd, J = 5, 8 Hz, 1H, CH-N), 3.36–3.28 (m, 2H, CH$_2$-N), 3.05–2.96 (m, 2H, CH$_2$-CONH), 2.91 (t, J = 8 Hz, 2H, CH$_2$-N), 1.93 (s, 3H, CH$_3$), 1.78–1.18 (m, 8H, CH$_2$); ^{13}C-NMR (D$_2$O): δ 179.06 (C=O), 173.53 (C=O), 170.50 (C=O), 148.81 (q, J = 18 Hz, SF$_5$), 142.44 (Ar-NH), 140.66 (Ar-SF$_5$), 131.17 (Ar), 126.88 (quin, J = 4 Hz, SF$_5$), 120.16 (Ar), 54.89 (CH-N), 48.84 (CH$_2$-N), 47.44 (CH$_2$-N), 42.92 (CH$_2$-CONH), 31.01 (CH$_2$), 26.29 (CH$_2$), 24.97 (CH$_2$), 22.07 (CH$_3$); ^{19}F-NMR (D$_2$O): δ 85.65 (m, 1F), 63.10 (d, J = 160 Hz, 4F).

3.6. 2-[[(2S)-2-(Acetylamino)-6-((2-carboxyethyl)amino)-[(4-trifluoromethylphenyl)amino]-4-hexanoic Acid (6b)

Compound **6b** was obtained as a transparent oil (71 mg, 0.178 mmol, 89%). HRMS (EI) Calcd for C$_{18}$H$_{23}$F$_3$N$_3$O$_4$ [M-H]$^-$ 402.1640, [M-H]$^-$ Found 402.1641; IR (KBr): 3273, 1606, 1548, 1409, 1324, 1162, 1112, 1067, 1016, 841, 510 cm^{-1}; ^{1}H-NMR (MeOD): δ 7.56–7.49 (m, 4H, Ar), 4.15 (dd, J = 5, 8 Hz, 1H, CH-N), 3.39–3.35 (m, 2H, CH$_2$-N), 3.07 (m, 2H, CH$_2$-CONH), 2.88 (t, J = 8 Hz, 2H, CH$_2$-N), 1.90 (s, 3H, CH$_3$), 1.74–1.06 (m, 8H, CH$_2$). ^{13}C-NMR (D$_6$-DMSO): ^{13}C-NMR (D$_6$-DMSO): δ 174.49 (C=O), 169.62 (C=O), 168.74 (C=O), 142.62 (Ar-NH), 127.95 (q, J = 5 Hz, CF$_3$), 119.35 (Ar), 119.08 (Ar), 47.41 (CH-N), 43.30 (CH$_2$-N), 33.87 (CH$_2$-N), 31.67 (CH$_2$-CONH), 31.50 (CH$_2$), 26.83 (CH$_2$), 26.49 (CH$_2$), 22.71 (CH$_3$); ^{19}F-NMR (D$_6$-DMSO): δ -59.78 (s, 3F).

3.7. 2-[[(2S)-2-(Acetylamino)-6-((2-carboxyethyl)amino)-[(phenyl)amino]-4-hexanoic Acid (6c)

Compound **6c** was obtained as a transparent oil (42 mg, 0.128 mmol, 64%). HRMS (EI) Calcd for C$_{17}$H$_{24}$N$_3$O$_4$ [M-H]$^-$ 334.1766, [M-H]$^-$ Found 334.1770; IR (KBr): 3295, 2945, 1560, 1499, 1444, 1399, 1311, 757, 693, 626, 560, 460 cm^{-1}; ^{1}H-NMR (D$_6$-DMSO): δ 7.59 (d, J = 7.6 Hz, 2H, Ar), 7.29 (t, J = 8 Hz, 2H, Ar), 7.04 (t, J = 7.2 Hz, Ar), 4.13–4.08 (m, 1H, CH-N), 2.87 (t, J = 7.2, 2H, CH$_2$-N), 2.81 (t, J = 7.2, 2H, CH$_2$-CONH), 1.93 (s, 3H, CH$_3$), 1.68–1.29 (m, 8H, CH$_2$); ^{13}C-NMR (D$_6$-DMSO): δ 173.83 (C=O), 169.31 (C=O), 168.21 (C=O), 138.92 (Ar-NH), 128.75 (Ar), 123.36 (Ar), 119.18 (Ar), 51.90 (CH-N), 48.60 (CH$_2$-N), 46.77 (CH$_2$-N), 42.77 (CH$_2$-CONH), 30.62 (CH$_2$), 26.56 (CH$_2$), 25.21 (CH$_2$), 22.57 (CH$_3$)

3.8. 2-[[(2S)-2-(Acetylamino)-6-((2-carboxyethyl)amino)-[(4-methoxyphenyl)amino]-4-hexanoic Acid (6d)

Compound **6d** was obtained as a transparent oil (42 mg, 0.116 mmol, 58%). HRMS (EI) Calcd for C$_{18}$H$_{26}$N$_3$O$_5$ [M-H]$^-$ 364.1872, [M-H]$^-$ Found 364.1872; IR (KBr): 3275, 1607, 1551, 1409, 1324, 1113, 1068, 1016, 842, 596, 511 cm^{-1}; ^{1}H-NMR (D$_6$-DMSO): δ 7.49 (d, J = 8 Hz, 2H, Ar), 6.85 (d, J = 8 Hz, 2H, Ar), 3.91–3.86 (m, 1H, CH-N), 3.70 (s, 3H, O-CH$_3$), 2.90 (t, J = 8 Hz, 2H, CH$_2$-N), 2.71 (m, 2H, CH$_2$-CONH), 2.59 (t, J = 8 Hz, CH$_2$-N), 1.81 (s, 3H, CH$_3$) 1.64–1.22 (m, 8H, CH$_2$); ^{13}C-NMR (D$_2$O): δ 167.98 (C=O), 162.44 (C=O), 159.36 (C=O), 145.44 (Ar-OCH$_3$), 118.71 (Ar-NH), 112.75 (Ar), 103.33 (Ar), 44.44 (O-CH$_3$), 43.83 (CH-N), 43.78 (CH$_2$-N), 37.76 (CH$_2$-N), 36.31 (CH$_2$), 32.13 (CH$_2$), 28.14 (CH$_2$), 20.50 (CH$_3$).

4. Conclusions

The *N*-aryl maleimide derivatives proved to be effective prosthetic groups for bioconjugation. In addition to their impressive reactivity, the aryl -SF$_5$ moieties electron-withdrawing effect also proved beneficial, as it was found to promote thio-succinimide ring hydrolysis of the conjugate into a stable and irreversible thio-succinamic acid linker. On a synthetic scale, the model bioconjugation reactions afforded the desired conjugates in 80–96% yields. However, great difficulty was experienced in isolating the thio-succinamic acid conjugates from the respective maleamic acid. A primary goal of this investigation was to produce a robust acrylamide derivative that would be applicable for bioconjugation with a wide variety of target biomolecules. However, the hydrophobicity of the *N*-aryl acrylamide derivatives poses a significant limitation, as the predominant portions of these targets require partially aqueous conditions for solvation. Model bioconjugations performed on a synthetic scale with *N$_\alpha$*-acetyl-*L*-lysine were successful; however, when methanol was used as a solvent, the desired conjugates were obtained in 58–89% yields.

References

1. Klenner, M.A.; Pascali, G.; Zhang, B.; Massi, M.; Fraser, B.H. [18F/19F] Isotopic Exchange Radiolabeling of Pentafluorosulfanyl Groups. *J. Label Compd. Radiopharm.* **2019**, *62*, S214. [CrossRef]
2. Sheppard, W.A. The Electrical Effect of the Sulfur Pentafluoride Group. *J. Am. Chem. Soc.* **1962**, *84*, 3072–3076. [CrossRef]
3. Hansch, C.; Leo, A.; Taft, R.W. A Survey of Hammett Substituent Constants and Resonance and Field Parameters. *Chem. Rev.* **1991**, *91*, 165–195. [CrossRef]
4. Prinz, C.; Starke, L.; Ramspoth, T.-F.; Kerkering, J.; Riaño, V.M.; Paul, J.; Neuenschwander, M.; Oder, A.; Radetzki, S.; Adelhoefer, S.; et al. Pentafluorosulfanyl (SF5) as a Superior 19F Magnetic Resonance Reporter Group: Signal Detection and Biological Activity of Teriflunomide Derivatives. *ACS Sens.* **2021**, *6*, 3948–3956. [CrossRef]
5. Hiscocks, H.G.; Ung, A.T.; Pascali, G. Novel Strategy for Non-Aqueous Bioconjugation of Substituted Phenyl-1,2,4-triazole-3,5-dione Analogues. *Molecules* **2022**, *27*, 6667. [CrossRef] [PubMed]

6.   Ochtrop, P.; Hackenberger, C.P.R. Recent advances of thiol-selective bioconjugation reactions. *Curr. Opin. Chem. Biol.* **2020**, *58*, 28–36. [CrossRef] [PubMed]

7.   Awoonor-Williams, E.; Rowley, C.N. Evaluation of Methods for the Calculation of the pKa of Cysteine Residues in Proteins. *J. Chem. Theory Comput.* **2016**, *12*, 4662–4673. [CrossRef]

8.   Krenske, E.H.; Petter, R.C.; Houk, K.N. Kinetics and Thermodynamics of Reversible Thiol Additions to Mono- and Diactivated Michael Acceptors: Implications for the Design of Drugs That Bind Covalently to Cysteines. *J. Org. Chem.* **2016**, *81*, 11726–11733. [CrossRef]

9.   Alley, S.C.; Benjamin, D.R.; Jeffrey, S.C.; Okeley, N.M.; Meyer, D.L.; Sanderson, R.J.; Senter, P.D. Contribution of linker stability to the activities of anticancer immunoconjugates. *Bioconjugate Chem.* **2008**, *19*, 759–765. [CrossRef]

10.   Lewis, M.R.; Shively, J.E. Maleimidocysteineamido-DOTA derivatives: New reagents for radiometal chelate conjugation to antibody sulfhydryl groups undergo pH-dependent cleavage reactions. *Bioconjugate Chem.* **1998**, *9*, 72–86. [CrossRef]

11.   Ravasco, J.M.J.M.; Faustino, H.; Trindade, A.; Gois, P.M.P. Bioconjugation with Maleimides: A Useful Tool for Chemical Biology. *Chem.-A Eur. J.* **2019**, *25*, 43–59. [CrossRef] [PubMed]

12.   Szijj, P.A.; Bahou, C.; Chudasama, V. Minireview: Addressing the retro-Michael instability of maleimide bioconjugates. *Drug Discov. Today Technol.* **2018**, *30*, 27–34. [CrossRef] [PubMed]

13.   Christie, R.J.; Fleming, R.; Bezabeh, B.; Woods, R.; Mao, S.; Harper, J.; Joseph, A.; Wang, Q.; Xu, Z.-Q.; Wu, H.; et al. Stabilization of cysteine-linked antibody drug conjugates with N-aryl maleimides. *J. Control. Release* **2015**, *220*, 660–670. [CrossRef]

14.   Baldwin, A.D.; Kiick, K.L. Tunable degradation of maleimide-Thiol adducts in reducing environments. *Bioconjugate Chem.* **2011**, *22*, 1946–1953. [CrossRef]

15.   Fontaine, S.D.; Reid, R.; Robinson, L.; Ashley, G.W.; Santi, D.V. Long-term stabilization of maleimide-thiol conjugates. *Bioconjugate Chem.* **2015**, *26*, 145–152. [CrossRef]

16.   Lyon, R.P.; Setter, J.R.; Bovee, T.D.; Doronina, S.O.; Hunter, J.H.; Anderson, M.E.; Balasubramanian, C.L.; Duniho, S.M.; Leiske, C.I.; Li, F.; et al. Self-hydrolyzing maleimides improve the stability and pharmacological properties of antibody-drug conjugates. *Nat. Biotechnol.* **2014**, *32*, 1059–1062. [CrossRef]

17.   Isom, D.G.; Castañed, C.A.; Cannon, B.R.; García-Moreno, B.E. Large shifts in pKa values of lysine residues buried inside a protein. *Proc. Natl. Acad. Sci. USA* **2011**, *108*, 5260–5265. [CrossRef]

18.   Boike, L.; Henning, N.J.; Nomura, D.K. Advances in covalent drug discovery. *Nat. Rev. Drug Discov.* **2022**, *21*, 881–898. [CrossRef]

19.   De Vivo, M.; Masetti, M.; Bottegoni, G.; Cavalli, A. Role of Molecular Dynamics and Related Methods in Drug Discovery. *J. Med. Chem.* **2016**, *59*, 4035–4061. [CrossRef] [PubMed]

20.   Sauers, C.K. The Dehydration of N-Arylmaleamic Acids with Acetic Anhydride. *J. Org. Chem.* **1969**, *34*, 2275–2279. [CrossRef]

21.   Machida, M.; Machida, M.I.; Kanaoka, Y. Hydrolysis of N-Substituted Maleimides: Stability of Fluorescence Thiol Reagents in Aqueous Media. *Chem. Pharm. Bull.* **1977**, *25*, 2739–2743. [CrossRef]

22.   Liu, S. Radiolabeled cyclic RGD peptides as integrin αvβ 3-targeted radiotracers: Maximizing binding affinity via bivalency. *Bioconjugate Chem.* **2009**, *20*, 2199–2213. [CrossRef] [PubMed]

23.   Danhier, F.; Le Breton, A.; Préat, V. RGD-based strategies to target alpha(v) beta(3) integrin in cancer therapy and diagnosis. *Mol. Pharm.* **2012**, *9*, 2961–2973. [CrossRef]

24.   Kapp, T.G.; Rechenmacher, F.; Neubauer, S.; Maltsev, O.V.; Cavalcanti-Adam, E.A.; Zarka, R.; Reuning, U.; Notni, J.; Wester, H.-J.; Mas-Moruno, C.; et al. A comprehensive evaluation of the activity and selectivity profile of ligands for RGD-binding integrins. *Sci. Rep.* **2017**, *7*, 39805. [CrossRef] [PubMed]

25.   Watt, S.K.I.; Charlebois, J.G.; Rowley, C.N.; Keillor, J.W. A mechanistic study of thiol addition to N-phenylacrylamide. *Org. Biomol. Chem.* **2022**, *20*, 8898–8906. [CrossRef]

26.   Ranu, B.C.; Banerjee, S. Significant rate acceleration of the aza-Michael reaction in water. *Tetrahedron Lett.* **2007**, *48*, 141–143. [CrossRef]